APPLICATION OF STATIC VAR COMPENSATOR FOR VOLTAGE STABILITY ENHANCEMENT AND POWER LOSS REDUCTION IN POWER SYSTEM NETWORKS

ADEBISI O. I.[1*], ADEJUMOBI I. A.[2], OGUNBOWALE P. E.[3] and ADE-IKUESAN O. O.[4]

[1,2,3]Department of Electrical and Electronics Engineering, Federal University of Agriculture, Abeokuta, Ogun State, Nigeria
[4]Department of Electrical and Electronics Engineering, Olabisi Onabanjo University, Ago Iwoye, Ogun State, Nigeria
*Corresponding Author E-mail: adebisi.oluwaseun@yahoo.com

ABSTRACT

In power systems, the mismatch between electricity supply and demand has led to difficulty in maintaining the system voltages within the statutory limit, causing voltage stability problem and consequently poor power transfer. This work is an application of Static Var Compensator (SVC) for voltage stability enhancement and power loss reduction in power system networks using the standard IEEE 6, 14, and 30-bus power networks as case studies. Using MATLAB/PSAT software (version 2.1.9 'R2012a'), the Newton-Raphson power flow modeling the steady state conditions of the sample networks was simulated without and with SVC. The simulation results revealed that the voltage profiles of all the considered networks were enhanced and within acceptable limit of $0.95 \leq V_i \leq 1.05\ p.u.$ ***after compensation was applied. The system total real power losses of the considered IEEE 6, 14 and 30-bus power networks which were 7.88, 25.76 and 16.05 MW respectively without SVC reduced to 7.08, 24.42 and 15.88 MW respectively with SVC, giving 10.15, 5.20 and 1.06% reduction in total real real power loss respectively for the sample networks. These results showed that SVC as a compensating device is capable of enhancing voltage profile and reducing power loss if incorporated in power system networks.***

Keyword: Voltage stability, Power transfer, Static var compensator, Newton-Raphson power flow, PSAT software

INTRODUCTION

Electricity plays a significant role in the development of any economy. The inadequate supply of electricity to the meet the ever-growing demand has caused power systems to operate under highly stressed conditions (Reddy, 2013; Kalaivani and Kamaraj, 2012). These in turn have led to the difficulty in maintaining the system voltages within the acceptable limits and therefore voltage stability problem.

Voltage stability refers to the ability of a power system to maintain steady voltages at all the buses in the system after being subjected to a disturbance from a given initial operating condition (Reddy, 2013; Kalaivani and Kamaraj, 2012). A system enters a state of voltage instability when there is a disturbance, increase in load demand, or change in system condition and this can causes a progressive and uncontrollable decline in voltage. Voltage stability has today become an important area receiving great attention from power system engineers and researchers (Moh and Soe, 2016; Rahman and Tiwari, 2016; Reddy, 2013; Nagesh and Puttaswamy, 2012). It is a severe problem which steadily reaches operating limits imposed by economic and environment constraints (Moh and Soe, 2016). Voltage instability can result in generation tripping which also cause system breakdown (Ramanjaneyulu and Padma, 2014).

The major cause of voltage instability problem in power systems is the inability of satisfy the reactive power demand (Bhole and Nigam, 2015; Reddy, 2013; Kalaivani and Kamaraj, 2012). When the system is in a state of instability, voltage profile is affected and any drop in voltage profile is accompanied by increase in the reactive power demand. If the reactive powers demand is not met, it further causes decay of the bus voltage and this can lead to poor power transfer capability in the system with possible deficient equipment performance and damage. This therefore creates the need for compensating devices that can enhance and stabilize the system voltage profile by providing the required reactive power supports to the system. One of the most useful and versatile devices that can produce the desired compensation for the system is Static Var Compensator (SVC). Its ability for effective voltage control in power system networks has been investigated in seveal studies (Baheshwar and Pachori, 2015; Sardar and Chirsty, 2015; Mathew *et al.,* 2014, Oyedoja, 2014, Rahman and Islam, 2014; Siddiqui and Deb, 2013; Kour *et al.*, 2012; Sandesh and Shivendra, 2012; Porate *et al.*, 2009). SVC is a flexible alternating current transmission system (FACTS) which employs power electronics based principle to control the flow of reactive power flow of the system where it is connected. The basic function of

an SVC is to maintain the voltage of a particular bus at a desired level by means of reactive power compensation (Prity and Amit, 2013). It has been used for high performance steady state and transient voltage control compensation, damping power swings, improve transient stability and reduce system losses by optimized reactive power control (Ramanjaneyulu and Padma, 2014; Prity and Amit, 2013).

Therefore, the goal of this work is to apply of static var compensator for voltage stability enhancement of power system networks and examine the effect of such voltage stability enhancement on the power transfer capability of the system.

STATIC VAR COMPENSATOR AND ITS OPERATING PRINCIPLE

Static Var Compensator (SVC) is a shunt connected static var generator or absorber whose output is regulated to exchange capacitive or inductive current for voltage control or for improving system stability (Ramanjaneyulu and Padma, 2014; Prity and Amit, 2013; Singh *et al.*, 2012). The SVC regulates voltage at its terminals by controlling the amount of reactive power injected into or absorbed from the power system (Moh and Soe, 2016; Ramanjaneyulu and Padma, 2014). When the system voltage is low, the SVC generates reactive power (SVC capacitive) and when system voltage is high, it absorbs reactive power (SVC inductive). Hence, the operating principle of an SVC is based on generation of a varying amount of leading or lagging reactive power to the lagging or leading system. The basic configuration of an SVC is shown in Figure 1.

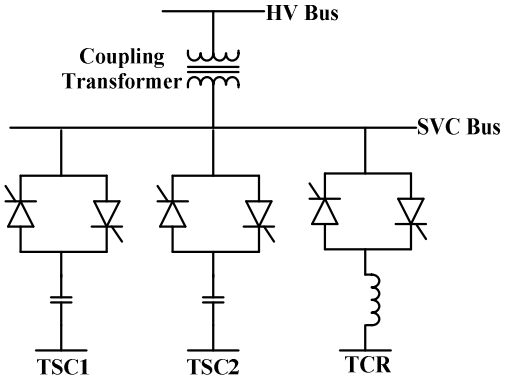

Figure 1: Basic configuration of a static var compensator (Moh and Soe, 2016)

In Figure 1, the SVC is connected to the ac bus whose voltage is to be controlled via a coupling transformer and switching of the three-phase capacitor banks and inductor banks connected on the secondary of the transformer allows the variation of the reactive power. The SVC comprises two thyristor switched capacitor (TSC) stages and a thyristor controlled reactor (TCR) stage. While leading vars are provided in the TSC stages, TCR stage provides the lagging vars. The lagging reactive power and TCR current amplitude can be controlled continuously by varying the thyristor firing angle between 90° and 180°. The TCR firing angle can be fully changed within one cycle of the fundamental frequency, therefore providing smooth and fast control of reactive power supply to the system (Moh and Soe, 2016). The leading vars are provided by a different number of capacitor bank units which are switched on or off in steps. The capacitor switching operation is completed within one cycle of the fundamental frequency and the TSC provides a faster and more reliable solution to capacitor switching (Moh and Soe, 2016). An alternative current filter is usually used to reduce and absorb the harmonic current components generated by TCR and hence, the leading vars are switched in steps and the lagging vars can be varied smoothly.

METHODOLOGY

In this section of the research work, the power flow formulation without and with inclusion of an SVC model is presented.

Formulation of the Power Flow Equations

Power flow refers to the flow active and reactive powers in power system networks. Power flow and bus voltage magnitudes with their phase anlges have bi-directional effects on each other. While the bus voltage magnitudes and their phase angles are affected by power flow in the networks, power flow in the transmission lines is also affected by the bus voltage magnitudes and their phase angles. Hence, the goal of power flow study is to provide such information as bus voltage magnitudes, bus voltage angles, active and reactive power flow through various branches, generators and loads under steady state conditions. These information are essential in evaluating the system performance and the effects of the proposed alternative plans on the system (Gupta, 2011).

Given a power system network comprising n buses, the current I_i injected at the ith bus in the system is expressed by equation (1) (Gupta, 2011; Kothari and Nagrath, 2008):

$$I_i = \sum_{k=1}^{n} Y_{ik} V_k \; ; \; i = 1, 2, \ldots . n \qquad (1)$$

where I_i = Current at ith bus

Y_{ik} = Admittance between bus *i* and bus *k*

V_k = Voltage at bus k

The complex power injected by the source into the ith bus is described by equations (2) and (3) which modify into equations (4) and (5) respectively with injected current I_i made the subject (Gupta, 2011; Kothari and Nagrath, 2008):

$$S_i = V_i I_i^* ; \; i = 1, 2, \ldots . n \qquad (2)$$

$$S_i = P_i + jQ_i \qquad (3)$$

$$I_i = \left(\frac{S_i}{V_i}\right)^* = \frac{S_i^*}{V_i^*} \qquad (4)$$

$$I_i = \frac{P_i - jQ_i}{V_i^*} \quad (5)$$

A simple cross multiplication in equation (5) results in equation (6) and the use of equation (1) in equation (6) yields equation (7):

$$P_i - jQ_i = V_i^* I_i \quad (6)$$

$$P_i - jQ_i = V_i^* (\sum_{k=1}^{n} Y_{ik} V_k); \; i = 1, 2, \ldots . n \quad (7)$$

The separation of equation (7) into real and imaginary components leads to equation (8) and (9) respectively:

$$P_i = Re\left(V_i^* (\sum_{k=1}^{n} Y_{ik} V_k)\right) \quad (8)$$

$$Q_i = -Im\left(V_i^* (\sum_{k=1}^{n} Y_{ik} V_k)\right) \quad (9)$$

where V_i, V_i^*, V_k and Y_{ik} are expressed in polar form as represented in equation (10).

$$\begin{cases} V_i = |V_i| e^{j\delta_i} \\ V_i^* = |V_i| e^{-j\delta_i} \\ V_k = |V_k| e^{j\delta_k} \\ Y_{ik} = |Y_{ik}| e^{j\theta_{ik}} \\ e^{j\varphi} = cos\varphi + jsin\varphi; \; \varphi = \delta_i, -\delta_i, \; \delta_k \; or \; \theta_{ik} \end{cases} \quad (10$$

The use of equation (10) in equations (8) and (9) respectively yields equations (11) and (12):

$$P_i = |V_i| \sum_{k=1}^{n} |Y_{ik}||V_k| \cos(\theta_{ik} + \delta_k - \delta_i) \quad (11)$$

$$Q_i = -|V_i| \sum_{k=1}^{n} |Y_{ik}||V_k| \sin(\theta_{ik} + \delta_k - \delta_i) \quad (12)$$

Equations (11) and (12) are called static power flow equations. Given n real and n reactive power flow equations, equations (11) and (12) together produce a total of 2n power flow equations. The unique feature of equations (11) and (12) is that they are both non-linear and therefore only numerical solution is possible. Varieties of numerical approaches are available for solving equations (11) and (12) but in this work, Newton-Raphson method is adopted because of its accuracy, reliability and faster rate of convergence (Gupta, 2011; Pabla, 2011; Kothari and Nagrath, 2008). The Newton-Raphson power flow is expressed by equation (12) (Gupta, 2011; Pabla, 2011; Kothari and Nagrath, 2008):

$$\begin{bmatrix} \Delta P \\ \Delta Q \end{bmatrix} = \begin{bmatrix} J_1 & J_2 \\ J_3 & J_4 \end{bmatrix} \begin{bmatrix} \Delta\delta \\ \Delta V \end{bmatrix} \quad (13)$$

where ΔP = Real power mismatch
ΔQ = Reactive power mismatch
ΔV = Bus voltage mismatch
$\Delta\delta$ = Bus voltage angle mismatch

J_1, J_2, J_3, and J_4 are the elements of Jacobian matrix which are obtained by partial differentiation of the equations (11) and (12) with respect to the state variables (δ, V). The off-diagonal and diagonal elements of J_1, J_2, J_3, and J_4 are as expressed in equations (14) to (21) (Gupta, 2011; Kothari and Nagrath, 2008):

The off-diagonal and diagonal elements of J_1:

$$\frac{\partial P_i}{\partial \delta_k} = V_i V_k Y_{ik} \sin(\theta_{ik} + \delta_i - \delta_k); \; k \neq i \quad (14)$$

$$\frac{\partial P_i}{\partial \delta_i} = -\sum_{\substack{k=1 \\ k \neq i}}^{n} V_i V_k Y_{ik} \sin(\theta_{ik} + \delta_i - \delta_k) \quad (15)$$

The off-diagonal and diagonal elements of J_2:

$$\frac{\partial P_i}{\partial V_k} = V_i Y_{ik} \cos(\theta_{ik} + \delta_i - \delta_k); k \neq i$$

$$\frac{\partial P_i}{\partial V_i} = 2V_i Y_{ii} \cos\theta_{ii} + \sum_{\substack{k=1 \\ k \neq i}}^{n} Y_{ik} V_k \cos(\theta_{ik} + \delta_i - \delta_k)$$

The off-diagonal and diagonal elements of J_3:

$$\frac{\partial Q_i}{\partial \delta_k} = -V_i V_k Y_{ik} \cos(\theta_{ik} + \delta_i - \delta_k); \; k \neq i \quad (18)$$

$$\frac{\partial Q_i}{\partial \delta_i} = \sum_{\substack{k=1 \\ k \neq i}}^{n} V_i V_k Y_{ik} \cos(\theta_{ik} + \delta_i - \delta_k) \quad (19)$$

The off-diagonal and diagonal elements of J_4:

$$\frac{\partial Q_i}{\partial V_k} = V_i Y_{ik} \sin(\theta_{ik} + \delta_i - \delta_k); k \neq i$$

$$\frac{\partial Q_i}{\partial V_i} = 2V_i Y_{ii} \sin\theta_{ii} + \sum_{\substack{k=1 \\ k \neq i}}^{n} Y_{ik} V_k \sin(\theta_{ik} + \delta_i - \delta_k)$$

The real and reactive power mismatches at each iteration with new estimates of bus voltage angles and bus voltage magnitude are expressed by equations (22) to (25):

$$\Delta P_i^r = P_i^{spec} - P_i^r$$

$$\Delta Q_i^r = Q_i^{spec} - Q_i^r$$

$$\delta_i^{r+1} = \delta_i^r - \Delta\delta_i^r$$

$$V_i^{r+1} = V_i^r - \Delta V_i^r$$

where r = iteration count

ΔP_i^r = Real power mismatch at iteration r

P_i^{spec} = Specified value of real power

P_i^r = Calculated value of real power at iteration r

ΔQ_i^r = Reactive power mismatch at iteration r

Q_i^{spec} = Specified value of reactive power

Q_i^r = Calculated value of reactive power at iteration r

δ_i^{r+1} = New estimate of bus voltage angle at iteration $r+1$

δ_i^r = Calculated value of bus voltage angle at iteration r

$\Delta\delta_i^r$ = Bus voltage angle mismatch at iteration r

V_i^{r+1} = New estimate of bus voltage at iteration $r+1$

V_i^r = Calculated value of bus voltage at iteration r

ΔV_i^r = Bus voltage mismatch at iteration r

The voltage and reactive power constraints at each bus i are given by equations (26) and (27) respectively:

$$V_{imin} \leq V_i \leq V_{imax} \quad (26)$$

$$Q_{imin} \leq Q_i \leq Q_{imax} \quad (26)$$

where V_{imin} = Minimum voltage value at bus i

V_{imax} = Maximum voltage value at bus i

Q_{imin} = Minimum reactive power supply at bus i

Q_{imax} = Maximum reactive power supply at bus i

Power Flow Models of SVC

Static var compensator is an automated impedance matching device designed to bring the system closer to unity power factor (Alok and Amar, 2012). It is usually shunt connected to provide fast response reactive power compensation, voltage control, improved system stability margin, damped system oscillations wherever they are desired in power networks through thyristorized switching elements (Nagendra *et al.*, 2015; Bahadur *et al.*, 2012). Basically, an SVC consists of a thyristor-controlled reactor (TCR) in parallel with a capacitor bank. The firing-angle control of thyristor enables the SVC to have very fast response (Bahadur *et al.*, 2012).

In order to analyse the reactive power compensation capability of an SVC, two models based on the concept of variable susceptance can be employed. These are variable shunt susceptance and firing angle models (Ramdan *et al.*, 2016; Bahadur *et al.*, 2012; Auchariyamet and Sirisumrannukul, 2010; Hassan *et al.*, 2009).

In the variable shunt susceptance model, the variable shunt susceptance is considered as the state variable in the power flow equations (Ramdan *et al.*, 2016; Bahadur *et al.*, 2012). The equivalent circuit of this model is shown in Figure 2. The current and reactive power equations along with the linearized Newton-Raphson power flow equations for this SVC model are expressed by equations (27) to (30) (Bahadur *et al.*, 2012):

$$I_{SVC} = B_{SVC} V_k \tag{27}$$

$$Q_{SVC} = Q_k = -V_k^2 B_{SVC} \tag{28}$$

$$\begin{bmatrix} \Delta P_k \\ \Delta Q_k \end{bmatrix}^{(r)} = \begin{bmatrix} 0 & 0 \\ 0 & Q_k \end{bmatrix}^{(r)} \begin{bmatrix} \Delta \delta_k \\ \Delta B_{SVC}/B_{SVC} \end{bmatrix}^{(r)} \tag{29}$$

$$B_{SVC}^{(r)} = B_{SVC}^{(r-1)} + \left(\frac{\Delta B_{SVC}}{B_{SVC}}\right)^{(r)} B_{SVC}^{(r-1)} \tag{30}$$

where I_{SVC} = Current drawn by SVC

B_{SVC} = Variable shunt susceptance of SVC

Q_{SVC} = Reactive power drawn by SVC which is also the reactive power injected by the SVC

ΔB_{SVC} = Variable shunt susceptance mismatch of SVC

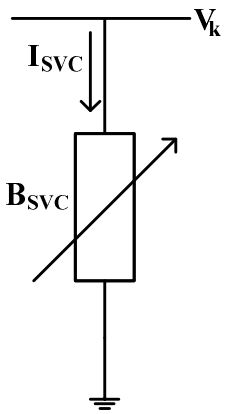

Figure 2: Variable shunt susceptance model of an SVC (Ramdan *et al.*, 2016; Bahadur *et al.*, 2012; Auchariyamet and Sirisumrannukul, 2010; Hassan *et al.*, 2009)

Equation (30) shows that the variable shunt susceptance B_{SVC} is updated at the end of the iteration (r). The total SVC susceptance is represented by this varying susceptance which is required to adjust the bus voltage to the prescribed value.

In the firing angle model, the firing angle, $\propto$, of the thyristor-controlled reactor (TCR) is considered as the state variable in the power flow equations (Ramdan *et al.*, 2016; Bahadur *et al.*, 2012). This model provides information on the SVC firing angel required to achieve a given level of compensation (Ramdan *et al.*, 2016). The equivalent circuit of the model is shown in Figure 3. The equivalent susceptance is a function of the changing firing angle. The susceptance and reactive power equations along with the linearized Newton-Raphson power flow equations for this SVC model are expressed by equations (31) to (34) (Bahadur *et al.*, 2012):

$$B_{SVC} = -\frac{\left\{X_L - \frac{X_C}{\pi}[2(\pi - \alpha_{SVC}) + \sin(2\alpha_{SVC})]\right\}}{X_C X_L} \tag{31}$$

$$Q_{SVC} = Q_k = \frac{V_k^2}{X_C X_L}\left\{X_L - \frac{X_C}{\pi}[2(\pi - \propto_{SVC}) + \sin(2 \propto_{SVC})]\right\} \tag{32}$$

$$\begin{bmatrix} \Delta P_k \\ \Delta Q_k \end{bmatrix}^{(r)} = \begin{bmatrix} 0 & 0 \\ 0 & \frac{2V_k^2}{\pi X_L}[\cos(2\alpha_{SVC}) - 1] \end{bmatrix}^{(r)} \begin{bmatrix} \Delta \delta_k \\ \Delta \propto_{SVC} \end{bmatrix}^{(r)} \tag{33}$$

$$\propto_{SVC}^{(r)} = \propto_{SVC}^{(r-1)} + \propto_{SVC}^{(r)} \tag{34}$$

where X_L = Inductive reactance

X_C = Capacitive reactance

$\propto_{SVC}$ = Firing angle of the SVC

$\Delta \propto_{SVC}$ = Firing angle mismatch of the SVC

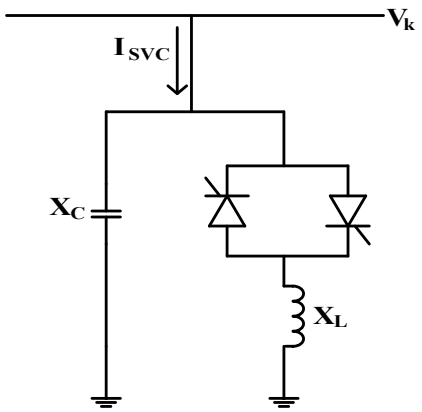

Figure 3: Firing angle model of an SVC (Ramdan *et al.*, 2016; Auchariyamet and Sirisumrannukul, 2010; Hassan *et al.*, 2009)

Equation (34) shows that the firing angle of the SVC is updated at the end of the iteration (*r*) and new susceptance can be computed from equation (31).

For the purpose of this work, firing angle model of an SVC is adopted. This is primarily because the model requires no additional iterative loop to solve for the firing angle unlike the variable shunt susceptance model (Bahadur *et al.*, 2012). The power flow equations of the model are combined with the system's power flow equations and linearized with respect to the state variables to obtain the complete power flow equations for the system including the SVC. The effect of incorporation of SVC into the system power flow equations is that the size of the Jacobian matrix increases to accommodate the partial derivatives of the SVC real and reactive powers withn respect to the state variables. Since the SVC consumes no real power, all the partial derivatives of its real power with respect to the state variables are zero.

Choice of Simulation Software

In this work, the simulation of the power flow equations developed was performed using MATLAB/PSAT software version 2.1.9 (R2012a). PSAT software is a full-featured graphical power flow program to create, examine and modify the power flow data, solve the power flow and view the solution report (Powertech, 2017). The power flow data and solution are displayed in tables as well as on diagrams. The software contains many useful features which facilitate design of single-line diagrams of various networks for analysis with the power flow data. It choice for this work was due to its simplicity, ease of use, efficiency and less calculation requirements.

Sample Networks

In order to examine the performance of static var compensator for voltage control action, the developed power flow equations were tested on three standard power system networks. These are IEEE 6, 14 and 30 bus power networks. One-line diagrams of the networks are respectively shown in Figures 4, 5 and 6 respectively while their network and generator data are in the appendices.

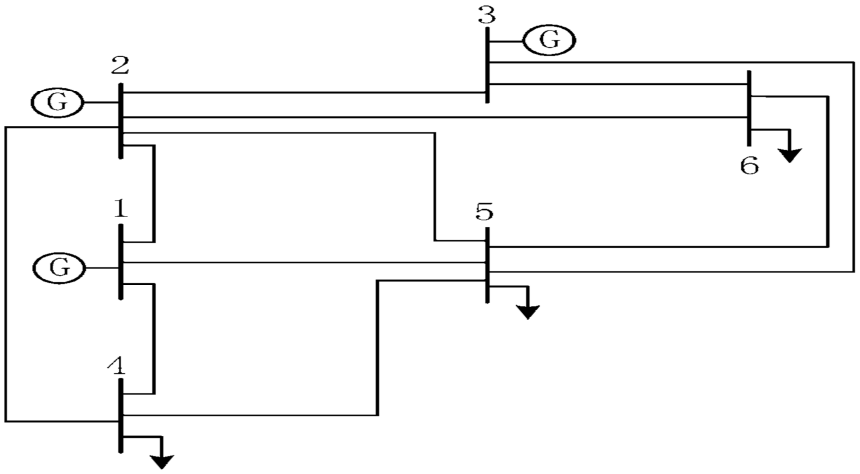

Figure 4: IEEE 6-bus power network (Shodhganga, 2017a)

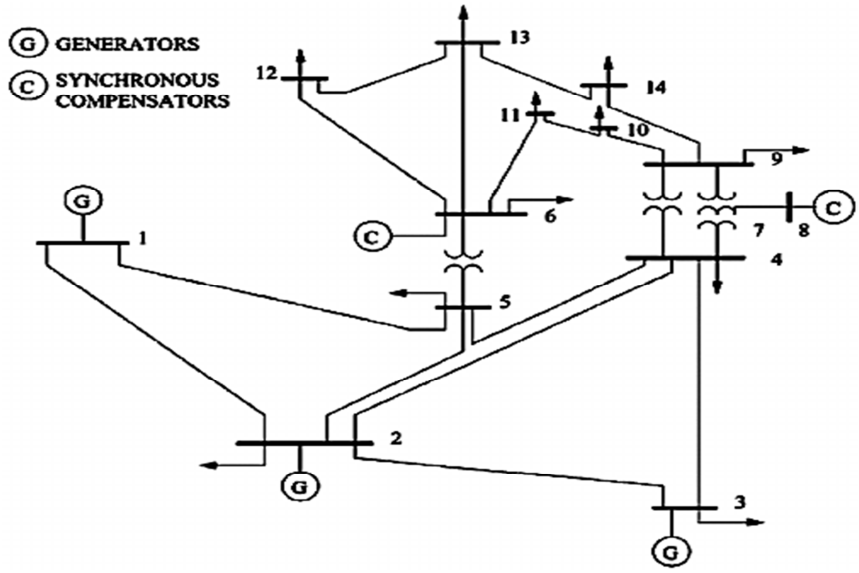

Figure 5: IEEE 14-bus power network (Shodhganga, 2017b)

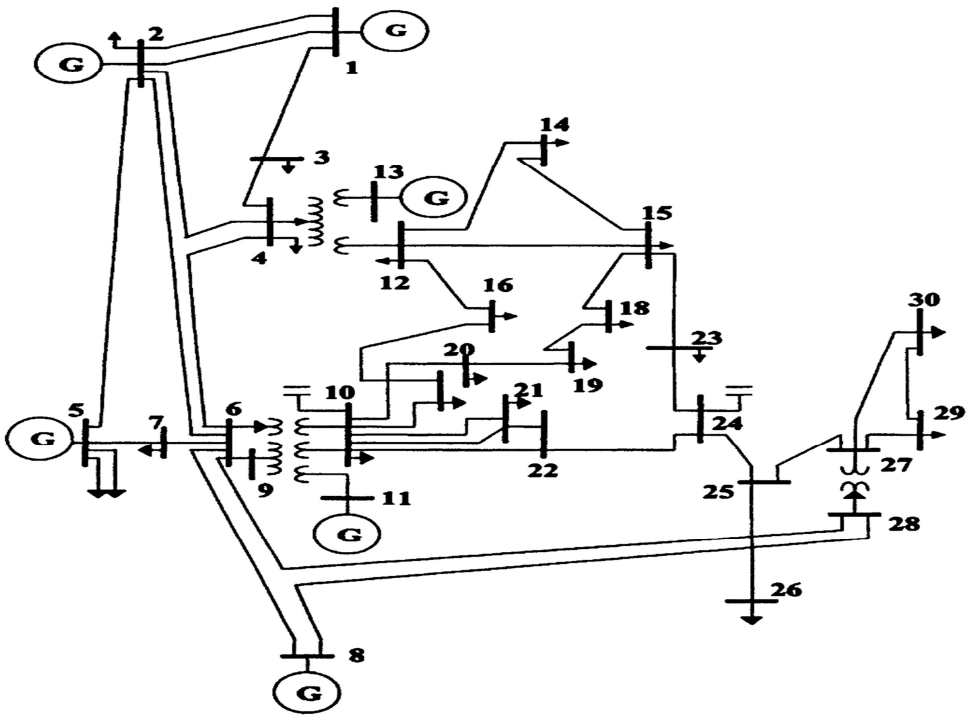

Figure 6: IEEE 30-bus power network (Shodhganga, 2017b)

RESULTS AND DISCUSSION

The simulation results without and with SVC are presented in this section. The parameters used for designing the firing-angle model of the SVC for the IEEE 6, 14 and 30-bus power systems considered as case studies for this work are presented in Table 1

.

Table 1: Parameters used for the SVC Design

Parameter	Value
Inductive reactance	0.75pu
Capacitive reactance	0.35pu
Reference voltage	1.0pu
Regulator time constant	10s
Regulator gain	100pu
Integral deviation constant	0.001pu
Transient time constant	0.05s
Measurement gain	1.000pu
Time delay	0.01s
Firing angle range	$pi/2 \leq \propto \leq pi$

Simulation Results of the IEEE 6-Bus Power Network

The PSAT models of the IEEE 6-bus power network without and with the inclusion of SVC are presented in Figure 7. The obtained system voltage profile and total active power loss from running the Newton-Raphson power flow simulation of the models in Figure 7 using the PSAT software are shown in Figures 8 and 9 respectively.

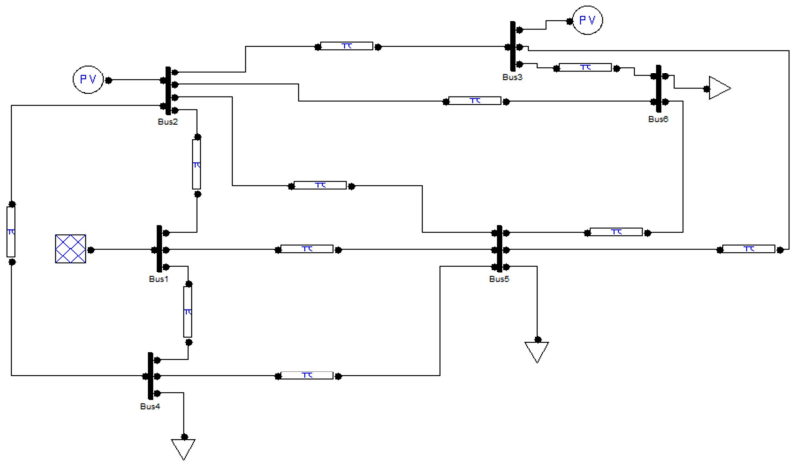

(a)

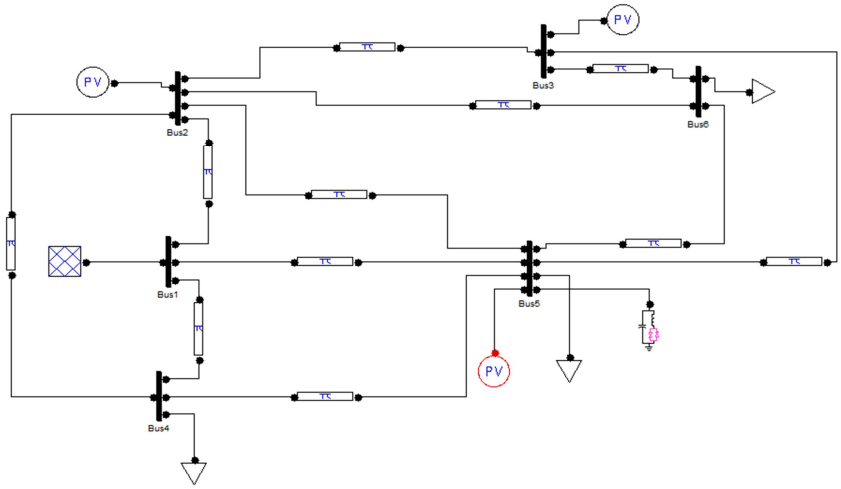

(b)

Figure 7: (a) PSAT model of the IEEE 6-bus power network without SVC (b) PSAT model of the IEEE 6-bus power network with SVC

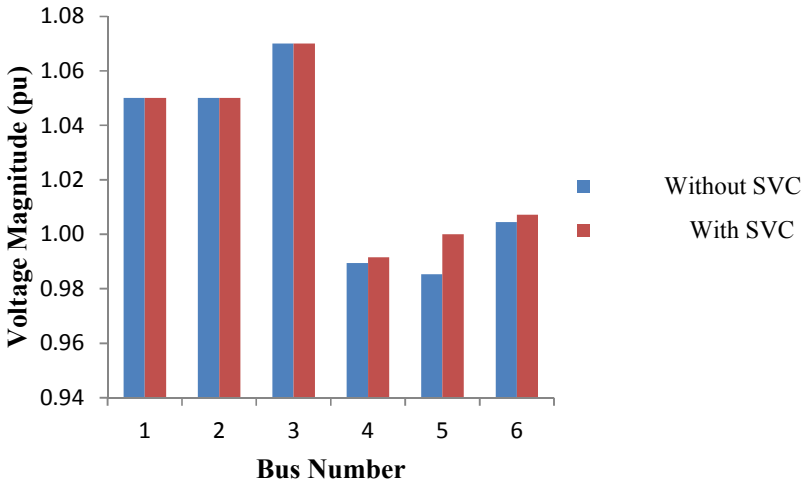

Figure 8: Bar chart showing the voltage magnitude of IEEE 6-bus power network without and with SVC

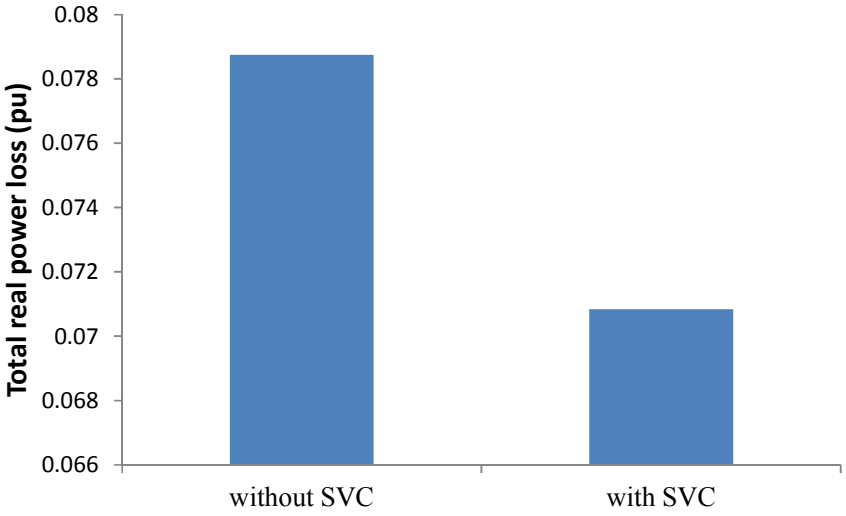

Figure 9: Bar chart showing the total real power loss of IEEE 6-bus power network without and with SVC

From Figure 8, it was observed that without compensation, the voltage magnitudes of all the buses in per unit (p.u.) fell within the statutory limit defined by $0.95 \leq V_i \leq 1.05$ p.u. However, when SVC was applied to the system, the voltage magnitudes of buses 4, 5 and 6 already within the statutory limit still improved respectively from 0.9894, 0.9854 and 1.0044 to 0.9915, 1.0000 and 1.0072 respectively. In Figure 9, it was shown that the system total real power loss which was 0.0788 p.u. (7.88 MW on MVA base 100) without compensation was reduced to 0.0708 p.u. (7.08 MW on MVA base 100) after SVC was applied. This in effect gave a 10.15% reduction in the system total real power loss.

Simulation Results of the IEEE 14-Bus Power Network

Figure 10 shows the PSAT models of the IEEE 14-bus power network without and with compensation. The system voltage profile and total active power loss obtained from the simulation of the Newton-Raphson power flow of the models in Figure 10 using PSAT software are shown in Figures 11 and 12 respectively.

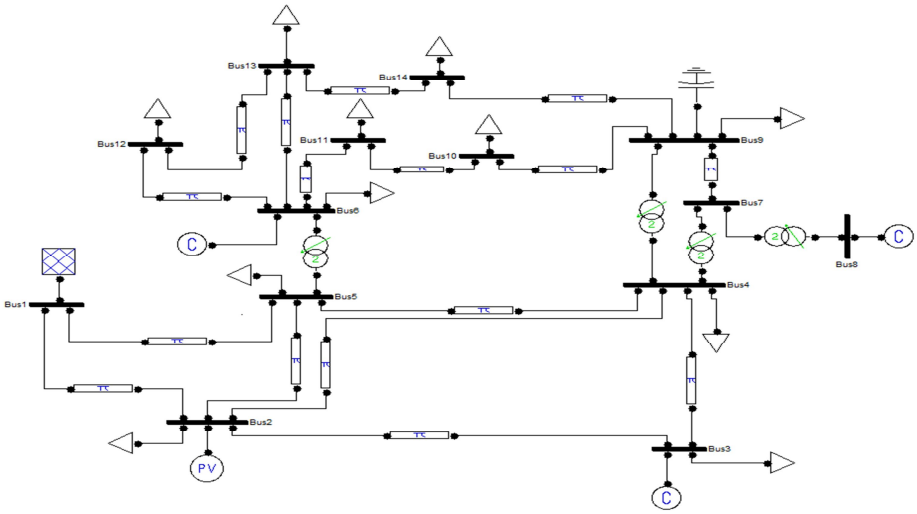

(a)

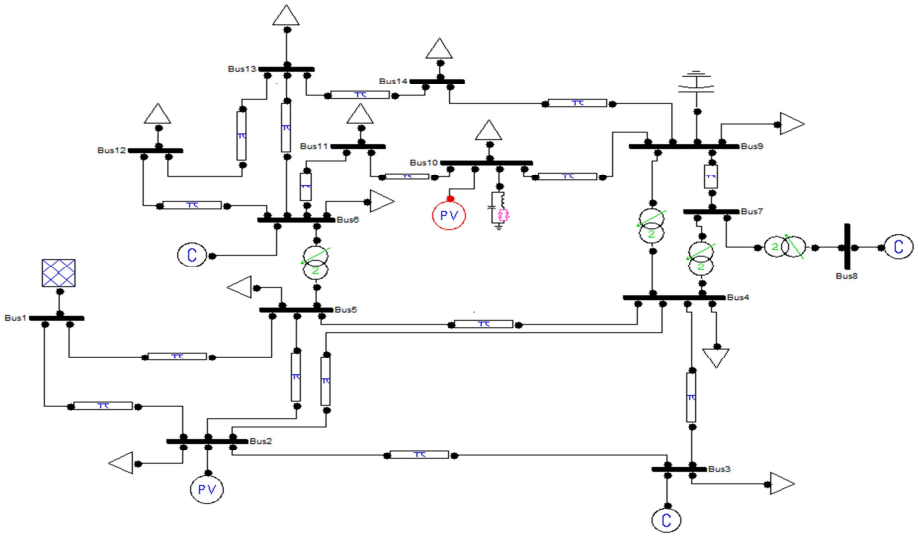

(b)

Figure 10: (a) PSAT model of the IEEE 14-bus power network without SVC (b) PSAT model of the IEEE 14-bus power system with SVC

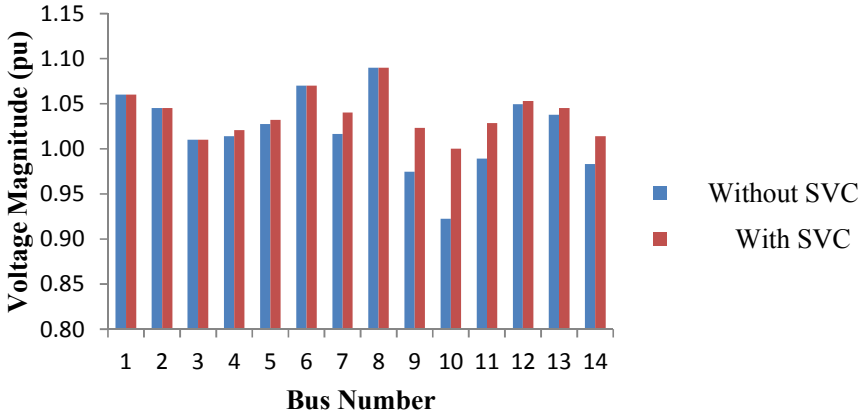

Figure 11: Bar chart showing the voltage magnitude of IEEE 14-bus power network without and with SVC

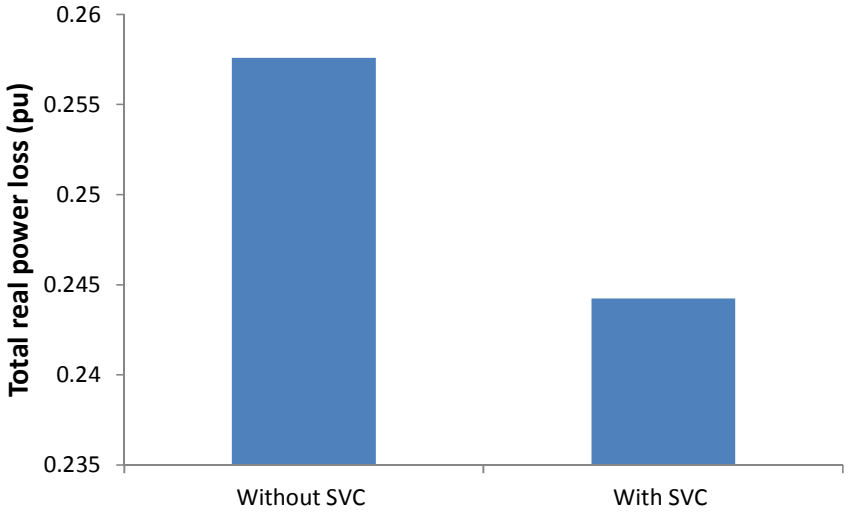

Figure 12: Bar chart showing the total real power loss of IEEE 14-bus power network without and with SVC

It was observed from Figure 11 that without compensation, the voltage magnitude of only bus 10 which was 0.9223 p.u. fell out of the statutory limit. However, when SVC was applied on the system, the voltage magnitude of bus 10 increased to 1.000 p.u. and the voltage magnitude of some other buses for example buses 9, 11 and 14 increased from 0.9747, 0.9892, 0.9831 to 1.0231, 1.0284 and 1.0140 respectively. This revealed that the voltage profile of the network was enhanced with the incorporation of SVC device. Similarly, the total real power loss of the system reduced from 0.2576 p.u. (25.76 MW on MVA base of 100) without SVC to 0.2442 p.u. (24.42 MW on MVA base of 100) with SVC included, giving percentage reduction of 5.20%.

Simulation Results of the IEEE 30-Bus Power Network

The PSAT models of the IEEE 30-bus power network without and with SVC is shown in Figure 13. Figures 14 and 15 respectively show the obtained system voltage profile and total active power loss from the simulation of the Newton-Raphson power flow of the models in Figure 13 using PSAT software.

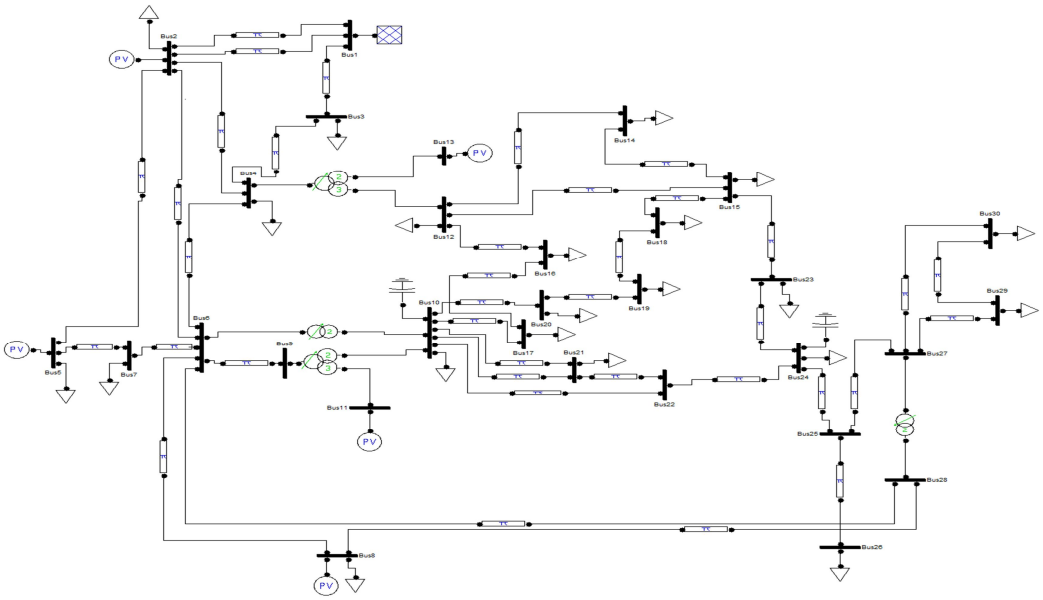

(a)

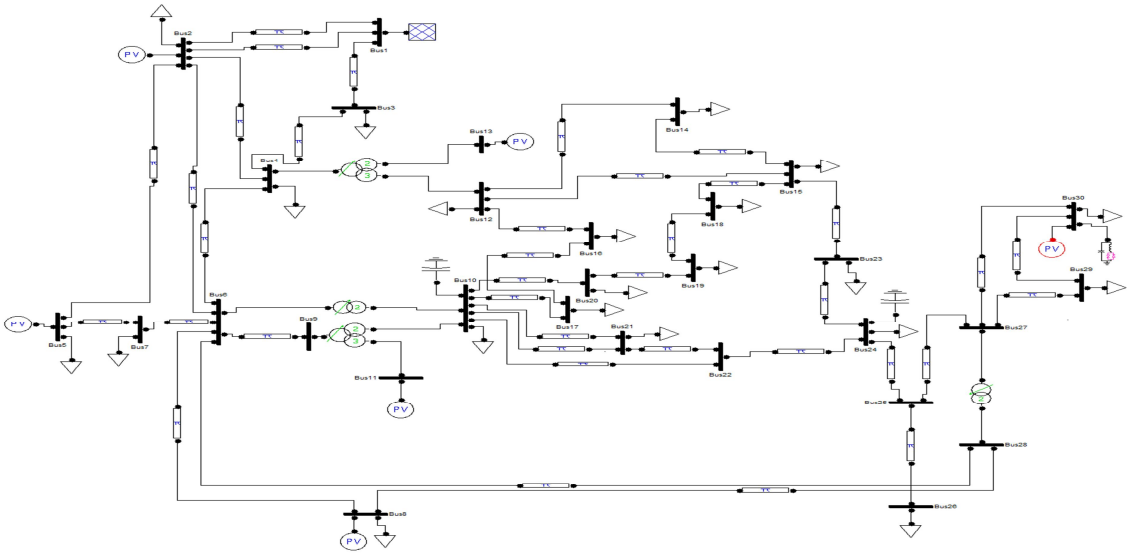

(b)

Figure 13: (a) PSAT model of the IEEE 30-bus power network without SVC (b) PSAT model of the IEEE 30-bus power system with SVC

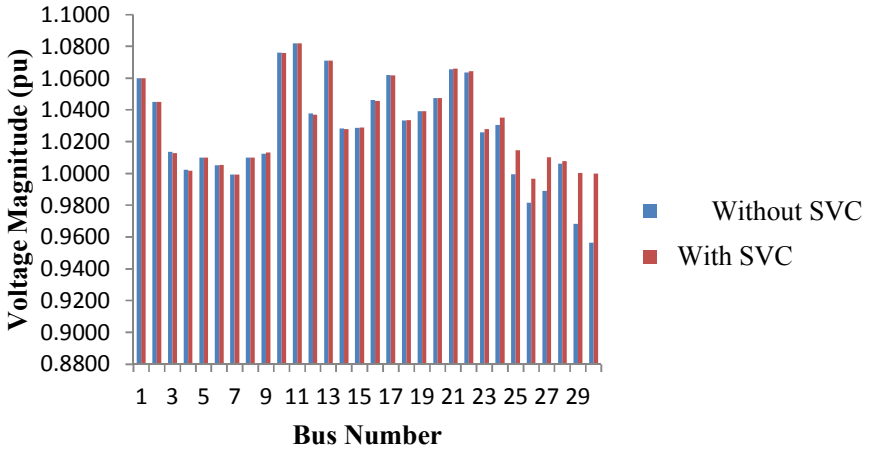

Figure 14: Bar chart showing the voltage magnitude of IEEE 30-bus power network without and with SVC

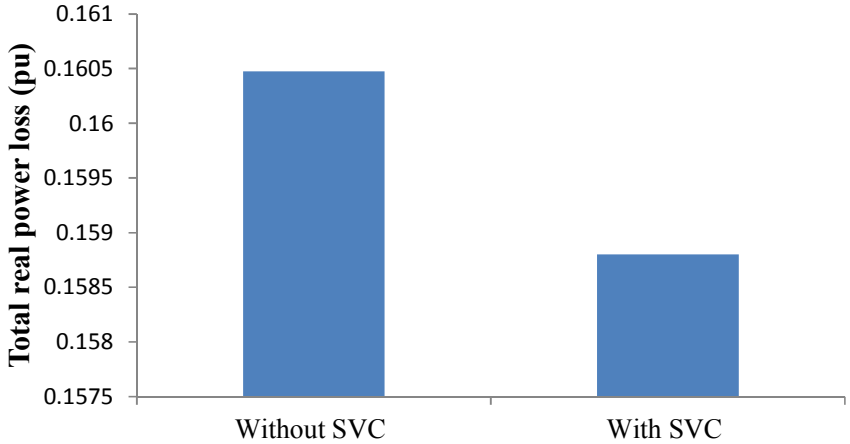

Figure 15: Bar chart showing the total real power loss of IEEE 30-bus power network without and with SVC

From the voltage profile shown in Figure 14, the voltage magnitude of all the buses were observed to be within the statutory limit when no

compensation was applied on the system. However, the inclusion of SVC despite the voltage magnitude of each of the buses falling within the statutory limit still enhanced the voltage profile of the system. For instance, the voltage magnitudes of buses 26, 27, 29 and 30 increased from 0.9815, 0.9890, 0.9684, 0.9565 p.u. to 0.9967, 1.0101, 1.0003 and 1.0000 p.u. respectively after compensation was applied on the network. More so, there is an improvement on the system line loss with SVC incorporated in the system. The system total real power loss reduced from 0.1605 p.u. (16.05 MW on MVA base of 100) without SVC to 0.1588 p.u. (15.88 MW on MVA base of 100) with SVC applied. This results in 1.06% reduction in the system total real power loss.

Analysis of SVC Performance on the Sample Networks

As observed from the simulation results of the PSAT models of the sample networks considered in this work, static var compensator has shown the capability to enhance the voltage profile of the network in which it is applied to acceptable limit and consequently minimises the system line losses. For sample networks considered, with SVC applied, the voltage magnitude of the bus outside the specified voltage limit of $0.95 \leq V_i \leq 1.05\ p.u.$ was improved to within the limit and the voltage magnitudes of some of the buses already within the specified limit were further enhanced. This signifies the voltage enhancement ability of the SVC in this work. Not only did the voltage profiles of the sample networks considered improved with the inclusion of SVC but the effect of these improvements in voltage profiles of the networks also reflected on the total real power losses of the transmission lines. For each of the sample network, the total real power loss which was previously high without SVC reduced appreciably with application of SVC. These results therefore revealed that SVC has the capability of enhancing the voltage stability and power loss in power system networks if incorporated.

CONCLUSION

Voltage stability and power loss reduction have today become two important factors that are crucial to an improved performance of power systems. In this work, static var compensator was applied for voltage stability enhancement and power loss reduction in power system networks using the standard IEEE 6, 14 and 30-bus power networks as case studies. The obtained results from Newton-Raphson power flow simulation on sample networks without and with SVC using MATLAB/PSAT software revealed that voltage profiles of all the considered networks were enhanced and within statutory limit of $0.95 \leq V_i \leq 1.05\ p.u.$ with the application of compensation. Equally, the effect of enhanced voltage profiles on the sample networks also reflected on the total real power loss of the systems. The total real power losses of IEEE 6, 14 and 30-bus power networks which were 7.88, 25.76 and 16.05 MW respectively without compensation reduced to 7.08, 24.42 and 15.88 MW respectively with compensation, giving 10.15, 5.20 and 1.06% reduction in total real real power loss respectively for the sample networks. These results showed that SVC is effective in enhancing the voltage stability and power loss of power system networks if employed as a compensating device.

REFERENCES

Alok, K.M. and Amar K.B. (2012). Power System Stability Improvement Using FACTS Devices. *International Journal of Modern Engineering Research, 1(2): 666-672.*

Bahadur, S.P., Suman, B. and Narendra, K. (2012). Power Flow Models of Static Var Compensator and Static Synchronous Compensator. Retrieved November 28, 2017 from https://www.researchgate.net/publication/261312122

Baheshwar, N and Pachori, A (2015). Voltage Profile Improvement Using Static VAR Componsator in Power System. *International Journal of Novel Research in Electrical and Mechanical Engineering, 2(2): 59-64.*

Bhole, S.S. and Nigam, P. (2015). Improvement of Voltage Stability in Power System By Using SVC and STATCOM. *International Journal of Advanced Research in Electrical, Electronics and Instrumentation Engineering, 4(2): 749-755.*

Gupta, J.B. (2011). A Course in Power Systems. S.K. Kataria and Sons Publisher, New Delhi, India.

Hassan, M.O., Cheng, S.J. and Zakaria, Z.A. (2009). Steady-State Modeling of SVC and TCSC for Power Flow Analysis. *Proceedings of the International Multi-Conference of Engineers and Computer Scientists, Vol. II, March 18-20, Hong Kong.*

Kalaivani, R. and Kamaraj, V. (2012). Enhancement of Voltage Stability by Optimal Location of Static Var Compensator Using Genetic Algorithm and Particle Swarm Optimization. *American Journal of Engineering and Applied Sciences, 5(1): 70-77.*

Kothari, D. P. and Nagrath, I. J. (2008), Power system engineering, Tata McGraw-Hill Publishing Company.

Kour, G., Brar, G.S. and Dhiman, J.. (2012). Improvement of Voltage Profile by Static Var Compensators in Distribution

Substation. *International Journal of Instrumentation Science, 1(2): 21-24.*

Matthew S., Wara S.T., Adejumobi I.A., Ajisegiri, E.S.A. and Olanipekun A.J. (2014). Power System's Voltage Stability Improvement Using Static Var Compensator. *International Journal of Emerging Technology and Advanced Engineering, 4(1): 494-501.*

Moh, M.M.A. and Soe, W.N. (2016). Voltage Stability Improvement Using Static Var Compensator with Fuzzy Logic Controller. *International Journal of Advanced Computational Engineering and Networking, 4(8): 51-56.*

Nagendra, P, Sunita, H.D and Subrata, P (2015). Location of Static Var Compensator in a Multi-Bus Power System Using Unique Network Equivalent. *Advances in Energy Research, 3(4): 235-249.*

Nagesh, H.B. and Puttaswamy, P.S. (2012). Power Flow Model of Static Var Compensator and Enhancement of Voltage Stability. *International Journal of Advances in Engineering and Technology, 3(2): 499-507.*

Oyedoja, K.O. (2014). Modeling and Simulation Study of the Use of Static Var Compensator (SVC) for Voltage Control in Nigeria Transmission Network. *International Journal of Engineering and Applied Sciences, 5(5): 44-50.*

Pabla, A.S. (2011). Electric power distribution. Tata McGraw-Hill, New Delhi, India.

Porate, K., Thakpe, K.L. and Boghe, G.L. (2009). Voltage Stability Enhancement of Low Voltage Radial Distribution Network Using Static Var Compensator: A Case Study. *WSEAS Transactions on Power Systems, 1(4): 32-41.*

Powertech (2017). PSAT User Manual. Retrived November 28, 2017 from www.powertechlabs.com.

Prity, B. and Amit, S. (2013). Comparison between SVC and STATCOM FACTS Devices for Power System Stability Enhancement. *International Journal of Emerging Technologies, 4(2): 101-109.*

Rahman, M.A and Islam, M.S (2014). Voltage Control and Dynamic Performance of Power Transmission Using Static Var Compensator. *International Journal of Interdisciplinary and Multidisciplinary Studies, 1(4): 141-151.*

Rahman, Z. and Tiwari, A. (2016). Enhancement of Voltage Profile by Using Static Synchronous Compensator in Power System Networks. *S-JPSET, 8(2): 109-120.*

Ramanjaneyulu, K.S. and Padma, K. (2014). Voltage Profile Enhancement in a Power System Based on SVC Control Strategy Using PSIM Software. *IMPACT: International Journal of Research in Engineering and Technology, 2(2): 213-222.*

Ramdan, G.M. Mulyadi, Y. and Hasbulla (2016). The Voltage Profile Improvement Using Static Var Compensator (SVC) in Power System Transmission. *IOP Conference Series: Materials Science and Engineering, Vol. 128, Conference 1.*

Reddy, D.V.B. (2013). Voltage Collapse Prediction and Voltage Stability Enhancement by Using Static Var Compensator. *International Journal of Engineering Research and Applications, 3(5): 798-805.*

Sandesh, J and Shivendra, S.T (2012). Voltage Control of Transmission System Using Static Var Compensator. *International Journal of Science and Engineering Applications, 1(2): 107-109.*

Sardar, R and Chirsty, A.A. (2015). Voltage Stability Improvement by Static Var Compensator. *International Journal of Science, Engineering and Technology Research, 4(5): 1347-1350.*

Siddiqui, A.S. and Deb, T (2013). Voltage Stability Enhancement through Static Var Compensator. *International Journal of Scientific and Engineering Research, 4(2): 1-8.*

Shodhganga (2017a). One-line diagram of IEEE 6-bus power network. Retrieved November 28, 2017 from shodhganga.inflibnet: http://shodhganga.inflibnet.ac.in/bitstream/10603/16900/13/13_appendix.pdf

Shodhganga (2017b). One-line diagrams of IEEE 14 and 30-bus power networks. Retrieved November 28, 2017 from shodhganga.inflibnet: http://shodhganga.inflibnet.ac.in/bitstream/10603/1271/18/18_appendix.pdf

Singh, S.K., Phunchok, L. and Sood, Y.R. (2012). Voltage Profile and Power Flow Enhancement with FACTS Controllers. *International Journal of Engineering Research and Technology, 1(5):1-5.*